

The Cryosphere Discuss., author comment AC2 https://doi.org/10.5194/tc-2021-156-AC2, 2021 © Author(s) 2021. This work is distributed under the Creative Commons Attribution 4.0 License.

Reply on RC2

Julien Meloche et al.

Author comment on "Characterizing tundra snow sub-pixel variability to improve brightness temperature estimation in satellite SWE retrievals" by Julien Meloche et al., The Cryosphere Discuss., https://doi.org/10.5194/tc-2021-156-AC2, 2021

Reviewer: 2

R2.C1 Line 120, could you provide more details in the ocean/lake effect removal? Although the SSMIS observations has been downscaled to 3.125 km resolution, however considering the bigger footprint of 36.5 GHz (4*6 km^2), can the water effect truly be excluded in the pixels near the ocean/lake? As can be seen from Figure 1, at CB for example, there are truly only a few grids that are lake free. How the influence of lake was considered?

Agreed, the influence of ocean or liquid water from deep lakes cannot be excluded if the pixel is 25 km (full resolution) from the coast. The snowpit area is within 25 km from the ocean so another area just outside 25 km was chosen. We skipped over this explanation originally. Our goal was to select a typical "arctic snow" area with so we could evaluate the CV_sd and DHF effect in PMW simulation. The following was added in section 2.3 to clarify water contribution.

For CB, an area with the same spatial coverage but a slightly different location was used since the snowpit area was within 25 km (resampled pixel resolution of SSMIS) from the ocean. The lakes in CB shown in Figure 1 were not considered in the soil emission contribution because most of the water was frozen (4-6) (Mironov et al., 2010), which had a similar permittivity to frozen soil (2-4) (Mavrovic et al., 2021) than liquid water. However, this simplification had importance for 19 GHz given that soil emission has a greater influence on the signal at this frequency, hence the composition of frozen water and soil derived from landcover information should be used instead. Since 37 GHz is more sensitive to snow volume scattering, this step was neglected. The 19 GHz frequency was briefly used in this study in Figure 7 (old version) only for TVC in 2018 to investigate the effect of snow variability which modifies the amount of snow scatterers inside the radiometer's footprint.

R2.C2 Line 120, also, the snowpit measurements were at point scale whereas the Tb data is at 3.1.25 km. Why and how the Tb data was averaged to match the point scale measurements? To which resolution was it averaged?

The following was added in section 2.3.

for both TVC and CB regions. A single value of measured T_B (per frequency) were used by averaging all pixels within snow pits area (CB: 24 pixels, TVC: 14 pixels for 37 GHz). Each pixel with at least one snow pit inside was used. Since all snow pits were aggregated to obtain mean value and distribution of snow properties for SMRT, averaged T_B covering the snow pits area was used.

R2.C3 Line 249: this line reads like the density and SSA of each of the two layers were estimated as a function of snow depth and DHF, too.

This sentence was removed for clarity.

R2.C4 To my understand, the DHF was determined only by one parameter, i.e., the snow depth. The prior information is the probability distribution of snow depth and the relationship between DHF and snow depth described in Figure 5. Therefore, the generated DHF (posterior DHF field) described in Figure 6 has also some random characteristics. In other words, Figure 6 is only a realization of DHF, one of the possibilities. The scatter points are not fixed, determined values. Therefore, will a different realization influence your TB simulation results?

Your understanding is correct. Different realizations are shown by the \pm 2 σ region in Figure 8 and 9. It is not explained in the text but the uncertainty (2 σ) is estimated by generating the same experiment of simulating T_B for the CV_sd range of 0.1 to 1 (basically Figure 7b) 20 times. The mean and std of those 20 simulations are shown by the middle line and the 2 σ range of those realizations.

.....

R2.C5 Figure 7, it will be more interesting to provide an estimation of distribution of TB difference between 18.7 and 36.5 GHz. The authors need to explain why the TBthat considers the sub-pixel variability is higher when the standard deviation of snow depth is higher. Is it because when the snow depth is higher, the reduced variability of DHF will result in less samples of strong volume scattering, such that the TB at 36.5 GHz will increase? In addition, will this result be influenced by the soil emission background?

We decided to briefly add 19 GHz in figure 7 (old version) so the small effect (negligeable) from CV on 19 GHz simulation could be shown. See addition from comment R2.C1 about soil contribution and the addition of 19 GHz in the data section. Figure 7 was updated so 37 and 19 GHz are both shown for TVC18.

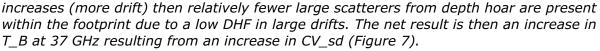
(see pdf for image)

This part was added to the result section 3.4.

The addition of snow variability in simulation (Figure 7 c-d) of 19 GHz has negligeable effect on T_B19 and showed a constant simulation across the CV_sd range of 0.1 to 1. Simulation of T_B19 showed higher biases at horizontal polarization then vertical polarization.

To address the second questions in the comment, the following paragraph was added in the discussion (section 4)

Considering that the difference between 19 and 37 GHz is used in SWE retrievals (Takala et al., 2011), using the CV_sd to account for variability of scatterers only affected simulation of 37 GHz with no effect on 19 GHz (Figure 7). If standard deviation of snow



R2.C6 How the effect of vegetation was considered in the simulation?

The effect of vegetation was not considered because it is not accounted in tundra snow retrievals (Saberi et al., 2020). Shrubs and tussock are not considered as trees or tall vegetation with significant interaction. Some studies do account for vegetation interaction with PMW but in sub-arctic areas with trees (Derksen et al., 2012; Larue et al., 2018; Roy et al., 2012). The interaction is based on vegetation product like Leaf Area Index which are not available for small vegetation like shrub.

R2.C7 Line 25: Snow depth simulations ---> do you mean the retrieved snow depth, or the brightness temperature simulations?

This sentence was modified.

SMRT simulations using a CV_sd of 0.9 best matched CV_sd observations [...]

R2.C8 Line 40: dielectric properties ---> suggested to change to radiometric properties

Modification done.

R2.C9 Line 75: More words is need to explain the Gaussian Process (GP) when this term first appears here. Maybe it is better to first mention it between lines 60-65.

The following sentence was modified by removing Gaussian Processes to avoid confusion.

which suggested the use of a term involving variation in snow depth and microstructure within the footprint instead of a uniform snow depth.

This sentence was also modified in the next introduction paragraph when stating the objectives of the study.

Finally, we perform a Gaussian Process fit to estimate depth hoar fraction (DHF) from snow depth, using probability density functions of snow depth to add variation of snow depth and microstructure within the footprint.

R2.C10 Line 81: are the snow microstructure and density values used here single values or probability distributions? Are they determined according to the in-situ snowpit observations?

We presented probability distributions of microstructure and density values, but single values (mean values) were used in the final simulation. The distributions are shown so they can be used in future MCMC retrievals as priors.

This sentence was modified as follows.

Secondly, we presented in situ measurements of snow microstructure and density in both

main tundra snow layers (depth hoar and wind slab), mean ratios of layer thickness and the depth hoar fraction (DHF) relative to snow depth.

R2.C11 Figure 5(b) was not described in the caption.

The following was added in the caption.

b) DHF is shown as a function of NVDI from the snowpit area with the mean DHF and NDVI shown by dashed lines and the gaussian distributions of DHF by the solid lines.

References

Derksen, C., Toose, P., Lemmetyinen, J., Pulliainen, J., Langlois, A., Rutter, N., Fuller, M.C., 2012. Evaluation of passive microwave brightness temperature simulations and snow water equivalent retrievals through a winter season. Remote Sens. Environ. 117, 236–248. https://doi.org/10.1016/j.rse.2011.09.021

Kim, R.S., Kumar, S., Vuyovich, C., Houser, P., Lundquist, J., Mudryk, L., Durand, M., Barros, A., Kim, E.J., Forman, B.A., Gutmann, E.D., Wrzesien, M.L., Garnaud, C., Sandells, M., Marshall, H.-P., Cristea, N., Pflug, J.M., Johnston, J., Cao, Y., Mocko, D., Wang, S., 2021. Snow Ensemble Uncertainty Project (SEUP): quantification of snow water equivalent uncertainty across North America via ensemble land surface modeling. Cryosph. 15, 771–791. https://doi.org/10.5194/tc-15-771-2021

King, J., Derksen, C., Toose, P., Langlois, A., Larsen, C., Lemmetyinen, J., Marsh, P., Montpetit, B., Roy, A., Rutter, N., Sturm, M., 2018. The influence of snow microstructure on dual-frequency radar measurements in a tundra environment. Remote Sens. Environ. 215, 242–254. https://doi.org/10.1016/j.rse.2018.05.028

Larue, F., Royer, A., De Sève, D., Roy, A., Cosme, E., 2018. Assimilation of passive microwave AMSR-2 satellite observations in a snowpack evolution model over northeastern Canada. Hydrol. Earth Syst. Sci. 22, 5711–5734. https://doi.org/10.5194/hess-22-5711-2018

Liston, G.E., Sturm, M., 1998. A snow-transport model for complex terrain. J. Glaciol. https://doi.org/10.1017/S0022143000002021

Marsh, P., Bartlett, P., MacKay, M., Pohl, S., Lantz, T., 2010. Snowmelt energetics at a shrub tundra site in the western Canadian Arctic. Hydrol. Process. 24, 3603–3620. https://doi.org/10.1002/hyp.7786

Mavrovic, A., Pardo Lara, R., Berg, A., Demontoux, F., Royer, A., Roy, A., 2021. Soil dielectric characterization during freeze-Thaw transitions using L-band coaxial and soil moisture probes. Hydrol. Earth Syst. Sci. 25, 1117–1131. https://doi.org/10.5194/hess-25-1117-2021

Mironov, V.L., De Roo, R.D., Savin, I. V., 2010. Temperature-dependable microwave dielectric model for an arctic soil. IEEE Trans. Geosci. Remote Sens. 48, 2544–2556. https://doi.org/10.1109/TGRS.2010.2040034

Parr, C., Sturm, M., Larsen, C., 2020. Snowdrift Landscape Patterns: An Arctic Investigation. Water Resour. Res. 56. https://doi.org/10.1029/2020WR027823

- Pomeroy, J.W., Gray, D.M., Hedstrom, N.R., Janowicz, J.R., 2002. Prediction of seasonal snow accumulation in cold climate forests. Hydrol. Process. 16, 3543–3558. https://doi.org/10.1002/hyp.1228
- Pulliainen, J., Luojus, K., Derksen, C., Mudryk, L., Lemmetyinen, J., Salminen, M., Ikonen, J., Takala, M., Cohen, J., Smolander, T., Norberg, J., 2020. Patterns and trends of Northern Hemisphere snow mass from 1980 to 2018. Nature 581, 294–298. https://doi.org/10.1038/s41586-020-2258-0
- Roy, A., Royer, A., Wigneron, J.-P., Langlois, A., Bergeron, J., Cliche, P., 2012. A simple parameterization for a boreal forest radiative transfer model at microwave frequencies. Remote Sens. Environ. 124, 371–383. https://doi.org/10.1016/j.rse.2012.05.020
- Royer, A., Domine, F., Roy, A., Langlois, A., Marchand, N., Davesne, G., 2021. New northern snowpack classification linked to vegetation cover on a latitudinal mega-transect across northeastern Canada. Écoscience 00, 1–18. https://doi.org/10.1080/11956860.2021.1898775
- Rutter, N., Sandells, M.J., Derksen, C., King, J., Toose, P., Wake, L., Watts, T., Essery, R., Roy, A., Royer, A., Marsh, P., Larsen, C., Sturm, M., 2019. Effect of snow microstructure variability on Ku-band radar snow water equivalent retrievals. Cryosph. 13, 3045–3059. https://doi.org/10.5194/tc-13-3045-2019
- Saberi, N., Kelly, R., Pan, J., Durand, M., Goh, J., Scott, K.A., 2020. The Use of a Monte Carlo Markov Chain Method for Snow-Depth Retrievals: A Case Study Based on Airborne Microwave Observations and Emission Modeling Experiments of Tundra Snow. IEEE Trans. Geosci. Remote Sens. 1–14. https://doi.org/10.1109/TGRS.2020.3004594
- Saberi, N., Kelly, R., Toose, P., Roy, A., Derksen, C., 2017. Modeling the observed microwave emission from shallow multi-layer Tundra Snow using DMRT-ML. Remote Sens. 9. https://doi.org/10.3390/rs9121327
- Sturm, M., Derksen, C., Liston, G., Silis, A., Solie, D., Holmgren, J., Huntington, H., 2008. A Reconnaissance Snow Survey across Northwest Territories and Nunavut, Canada, April 2007.
- Sturm, M., McFadden, J.P., Liston, G.E., Stuart Chapin, F., Racine, C.H., Holmgren, J., 2001. Snow-shrub interactions in Arctic Tundra: A hypothesis with climatic implications. J. Clim. https://doi.org/10.1175/1520-0442(2001)014<0336:SSIIAT>2.0.CO;2
- Takala, M., Luojus, K., Pulliainen, J., Derksen, C., Lemmetyinen, J., Kärnä, J.P., Koskinen, J., Bojkov, B., 2011. Estimating northern hemisphere snow water equivalent for climate research through assimilation of space-borne radiometer data and ground-based measurements. Remote Sens. Environ. https://doi.org/10.1016/j.rse.2011.08.014
- Walker, B., Wilcox, E.J., Marsh, P., 2020. Accuracy assessment of late winter snow depth mapping for tundra environments using Structure-from-Motion photogrammetry. Arct. Sci. 17, 1–17. https://doi.org/10.1139/as-2020-0006